

$$\frac{\partial p}{\partial x_1} = \frac{\partial \tau_{13}}{\partial x_3} \tag{2A}$$

and the continuity equation

$$\int_{x_3=0}^{x_3=h(x_1)} u_1 dx_3 = Q = \text{constant} \tag{3A}$$

are solved as follows.

Integrating equation (2A) with respect to x_3 gives,

$$\tau_{13} = \frac{dp}{dx_1} x_3 + F(x_1) \tag{4A}$$

where

$$F(x_1) = \tau_1(x_1).$$

Then substituting equation (4A) into equation (1A) results in

$$\frac{du_1}{dx_3} = \frac{\tau_L}{\mu} \tanh^{-1} \left[\left(\frac{dp}{dx_1} x_3 + F(x_1) \right) / \tau_L \right]. \tag{5A}$$

it is clear from equation (5A) that for $dp/dx_1 = 0$, the velocity u_1 is a linear function of x_3 , which with the no slip boundary conditions gives the flowrate $Q = (u_{11} + u_{21})/2h_0$. This is the same result as found with the usual Newtonian model [4]. Integrating equation (5A) from surface I with respect to x_3 gives the velocity distribution

$$u_1(x_3) - u_{11} = \frac{\tau_L^2}{2\mu p'} \left[\left(1 + \frac{p'x_3 + F}{\tau_L} \right) \ln \left(1 + \frac{p'x_3 + F}{\tau_L} \right) - \left(1 + \frac{F}{\tau_L} \right) \ln \left(1 + \frac{F}{\tau_L} \right) + \left(1 - \frac{p'x_3 + F}{\tau_L} \right) \ln \left(1 - \frac{p'x_3 + F}{\tau_L} \right) - \left(1 - \frac{F}{\tau_L} \right) \ln \left(1 - \frac{F}{\tau_L} \right) \right] \tag{6A}$$

If $x_3 = h$, then $u_1 = u_{21}$ and it will be the equation (3a) of the text.

Integrating the velocity distribution, equation (6A), in continuity, equation (3A) will result in equation (3b) of the text.

DISCUSSION

H. S. Cheng¹

The authors have added a valuable contribution to our knowledge of film formation of EHD contacts. They have demonstrated that for ordinary lubricants, whose limiting shear stress is far greater than that of 5P4E, the film formation is largely governed by the Newtonian behavior, and is not significantly affected by the limiting shear behavior of the lubricant at high pressures.

While this work seems to give us a greater confidence in applying current Newtonian EHD theories for the inlet film thickness, we must keep in mind that the film shape within the conjunction may be influenced to a much greater extent by non-Newtonian effects than the inlet behavior for high sliding contacts.

Let us take a simple sliding case for which the thermal effects would be strong and for which the stationary surface would be a much higher temperature than the moving surface. Under this condition, the velocity profile would change from a triangle profile at the inlet of the conjunction to a nearly rectangle shape at the center of the conjunction, owing to the lower limiting shear stress at a higher temperature. This action would greatly reduce the film thickness at the center of the conjunction. An analysis within the conjunction, which is much more involved than the Grubin-type analysis, appears to be needed for determining the full influence of the limiting shear effect on the minimum film thickness.

B. K. Daniels²

Non-Newtonian flow due to high stress is becoming an increasingly successful concept in explaining traction behavior. It is stimulating to see that the authors have already started to apply the concept to the inlet region of the contact. Such studies could be useful both in explaining film breakdown under high traction conditions and also in predicting any small contribution to traction that might be made outside the Hertzian zone. Such contributions could be important in highly conforming traction contacts running under low pressure with a high traction lubricant when efficiency is of prime importance.

As a first step the authors have completed a purely theoretical analysis of the line contact case. They have found that the reduction

of film thickness is only about 40 percent at slide roll ratios of 2. In traction drives the slide-roll ratio seldom exceeds .05 but outside the Hertzian zone of high spin contacts the local slide-roll ratio could be much higher. It might be interesting to try to extend this work to spinning point contacts.

The major assumptions seem to be sound: the pressure changes along the length at the same rate the shear stress changes across the thickness, the total flow is the integral across the thickness of the

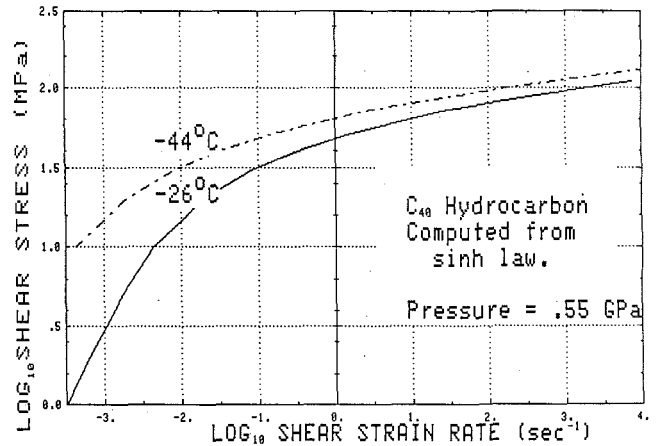


Fig. 16 Shear stress-strain behavior computed up to $10^{*}4 \text{ s}^{*-1}$ from the sinh law for 11,13-dioctyl-11 methyltricosane, $\alpha = \dots$ from, $\tau_{00} = 7 \text{ MPa}$ viscosity at atm press = \dots

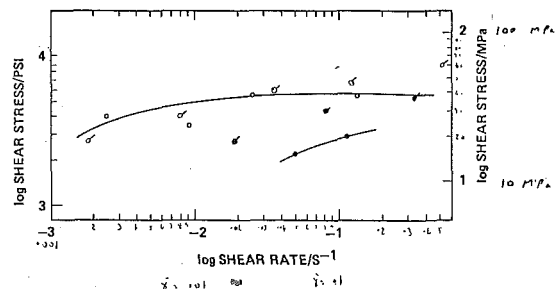


Fig. 17 Comparison of computed and measured shear stress-strain data for the same material and parameters as in Fig. 16

¹ Tokyo Institute of Technology, Ookayama, Meguro-Ku, Tokyo, Japan.

² Monsanto Co., St. Louis, Mo.

velocity, the elastic deformation of the steel is the same as without fluid, elastic deformation of the fluid is negligible compared to visco-plastic deformation, shear heating is negligible and the visco-plastic deformation follows a hyperbolic tangent law.

The last assumption was made because of the stress-strain behavior of very cold fluids at high pressure [12]. The shear stress leveled off to a remarkably constant value as the shear strain rate was increased several orders of magnitude. Fig. 16 shows that such a leveling off does not occur according to the sinh law which has been used for traction studies and which has a basis in rate theory. Note that the stress is plotted on a log scale. However, Fig. 17 shows that if parameters for the sinh law are taken from traction data and falling body pressure viscosity data the computed points, flagged, show approximate agreement with the experimentally measured data points. Those data are for linear branched aliphatic hydrocarbon (11,13-dioctyl-11 methyltricosane). The sinh law and the tanh law are therefore not very different from each other but the leveling of stress possible with the tanh law does seem to be strongly favored by the low temperature studies. An interesting future project would be to critically compare the sinh and tanh laws with experiments both on traction, that relates to inside the contact, on film thickness, that relates to conditions outside the contact, and on cold shearing. Another challenge, of course, is to explain the physical basis of the tanh law.

Additional Reference

12. Bair, S., and Winer, W. O., "Shear Strength Measurements of Lubricants at High Pressure," ASME Paper No. 78-Lub-9, Minneapolis Conference, Oct. 1978.

Authors' Closure

The analysis presented above covered several load, rolling and sliding conditions and viscosities but somewhat lacked in a presen-

tation of the direct relation between the film thickness and the limiting shear stress parameters, the curves given below complete this point of interest.

Effect of increasing the constant value of limiting shear stress for a particular slide/roll ratio; and tendency to approach a constant film thickness regardless of the slide/roll ratio at high slope m values are shown.

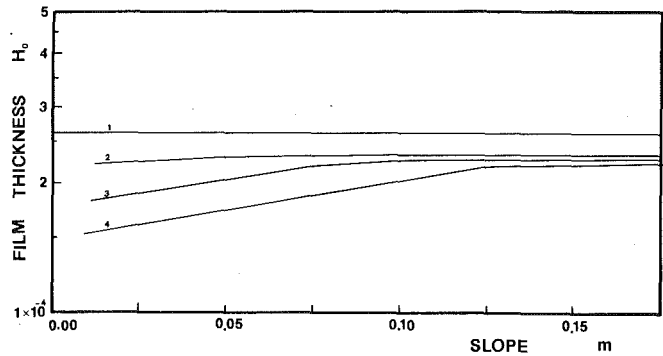


Fig. A Dimensionless film thickness versus slope of the limiting shear stress pressure relation

$$W/H = 87.6 \text{ k N/m (500 lb/in.)}$$

$$u_{11} + u_{21} = 2.54 \text{ m/s (100 in./sec)}$$

$$\mu_0 = 410 \text{ m Pas (5.94} \times 10^{-5} \text{ lb/in.}^2\text{)}$$

$$\tau_{L_0} = 0.69 \text{ m Pa (100 psi)}$$

- 1) Gubin's film thickness prediction
- 2) Model with $\Sigma = 0$
- 3) Model with $\Sigma = 1$
- 4) Model with $\Sigma = 2$

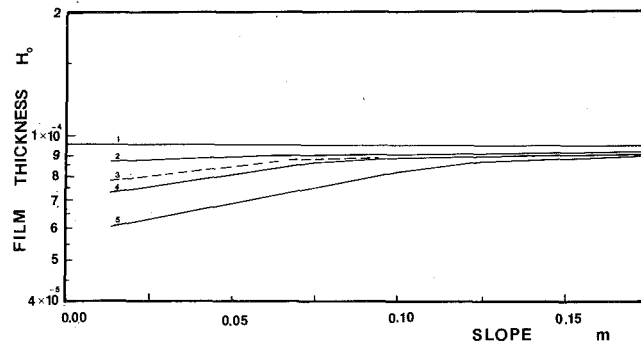


Fig. B Dimensionless film thickness versus slope of the limiting shear stress pressure relation

$$W/H = 876 \text{ kN/m (5000 lb/in.)}$$

$$u_{11} + u_{21} = 5 \text{ m/s (200 in./sec)}$$

$$\mu_0 = 69 \text{ m Pas (1} \times 10^{-5} \text{ lb/in.}^2\text{)}$$

$$\tau_{L_0} = 0.69 \text{ m Pa (100 psi) except for the case 3}$$

- 1) Grubin's film thickness prediction
- 2) Model with $\Sigma = 0$
- 3) Model with $\Sigma = 2$, and $\tau_{H_0} = 6.9 \text{ mPa (1000 pas)}$
- 4) Model with $\Sigma = 1$
- 5) Model with $\Sigma = 2$